An Improved Method for Deriving Daily Evapotranspiration Estimates From Satellite Estimates on Cloud-Free Days

Bingfang Wu, Weiwei Zhu, Nana Yan, Xueliang Feng, Qiang Xing, and Qifeng Zhuang

***Abstract*—An improved method, based on the daily surface resistance, is proposed to extend satellite evapotranspiration (ET) on a clear day into ET for each and every day. Alternative climatic variables such as soil moisture, wind speed, and net radiation are explored for estimating daily surface resistance using a Penman–Monteith (*P–M*) formulation. The study was carried out for the Yingke (YK) oasis plains area (maize cropland) and the Arou (AR) alpine meadow area (grassland) located in the midstream and upstream, respectively, of the Heihe River Basin of northwestern China. Statistical results show that the proposed method performs well for estimating daily ET for both study areas, with results slightly superior in the midstream, cropland area where the coefficient of determination (R^2) was 0.9249 and the index of agreement (d) was 0.978. In the upstream alpine meadow area, the coefficient of determination (R^2) was 0.9074, and the index of agreement (d) was 0.961. The proposed method provides an enhanced approach for estimating daily ET in the ETWatch model. Future work will focus on scaling this improved method to the estimation of regional daily ET map.**

***Index Terms*—Daily surface resistance, evapotranspiration (ET), ETWatch, Heihe river basin.**

I. Introduction

EVAPOTRANSPIRATION (ET) is an important component of the surface energy and water balance. Accurate estimation of ET is important for researchers in hydrology, meteorology, and agriculture including water resources management [1], the impact of climate change on water resources [2], and the planning of water-saving initiatives in irrigated areas [3], especially in arid and semiarid regions where water shortage is often a critical problem.

There are many methods to measure ET from either ground observation or remote sensing satellite data. Typically, ground observation requires advanced instrumentation and a high level of data screening and interpretation, and include lysimeters [4], Bowen ratio systems [5], eddy covariance (EC) systems, and large aperture scintillometers [6]–[8]. Although those methods are accurate for estimating ET at a single site or locally, using them at a larger regional scale is time consuming and expensive, requiring numerous ground installations when extensive spatial coverage and high sampling frequency are desired. To obtain ET at a regional scale, remote sensing methods are preferable.

Due to its space and time continuity and relatively low cost, remote sensing data are particularly useful for the study of regional-scale heterogeneous ET based on the surface energy balance. These data can be used to derive ET on a cloud-free day at the time of the daily satellite overpass at essentially every spatial location, which overcomes the spatial scale problem inherent in traditional ground-based observations. However, cloud cover prevents the collection of ET measures, but for water balance estimation and agricultural irrigation guidance, ET estimates are required for all days, not just those which are cloud free. Consequently, a "gap-filling" method is required to convert satellite overpass ET estimates on clear, cloud-free days into an ET estimates for each and every day irrespective of cloud cover, which we will refer to as daily ET

Since 1980, many methods have been proposed to scale a series of discontinuous and incomplete ET data into a complete daily ET, including the solar radiation ratio method [9], the reference ET fraction method [10]–[13], the Todorovic method [14]–[17], and the evaporative fraction method [18], [19]. The premise of all these methods is first to calculate on cloud-free days both the actual ET and the potential ET and assume that this proportion is the same on both cloud-free and cloudy days. Then, meteorological data are used to calculate potential ET, and actual ET for the cloudy days is estimated using this proportion. Those methods have performed well for estimating daily ET in a variety of environments [19]–[22]. However, these studies are generally limited to specific locations; it is more complex to estimate region-wide ET where a variety of underlying surfaces may exist.

Currently, the Penman–Monteith (*P–M*) model is most commonly used to convert satellite ET into complete daily ET [23]–[27]. This model has proved adequate for estimating the magnitude of ET flux variation in temperate and tropical ecosystems provided that the proper biophysical parameters are included [24], [28]–[30], such as daily reduction functions for stomatal aperture response to minimum air temperature m(T_{min}) and vapor pressure deficit m(VPD), smoothed leaf area index (LAI) values, and soil moisture content to estimate surface resistance. In actuality, many factors affect surface

Manuscript received July 23, 2014; revised December 20, 2015; accepted December 29, 2015. This work was supported in part by the Natural Science Foundation of China under Grant 41271424 and Grant 91025007 and in part by the Fund for Grains-Scientific Research in the Public Interest under Grant 201313009-2, and in part by the Found for Joint Program on Space Technology for Disaster Mitigation in Asia. (*Corresponding author: Bingfang Wu.*)

The authors are with the Division for Digital Agriculture, Key Laboratory of Digital Earth Science, Institute of Remote Sensing and Digital Earth, Chinese Academy of Sciences, Beijing 100101, China (e-mail: wubf@radi.ac.cn; zhuww@radi.ac.cn; yannn@radi.ac.cn; fengxl@radi.ac.cn; xingqiang@radi.ac.cn; zhuangqf@radi.ac.cn).

Color versions of one or more of the figures in this paper are available online at http://ieeexplore.ieee.org.

Digital Object Identifier 10.1109/JSTARS.2015.2514121

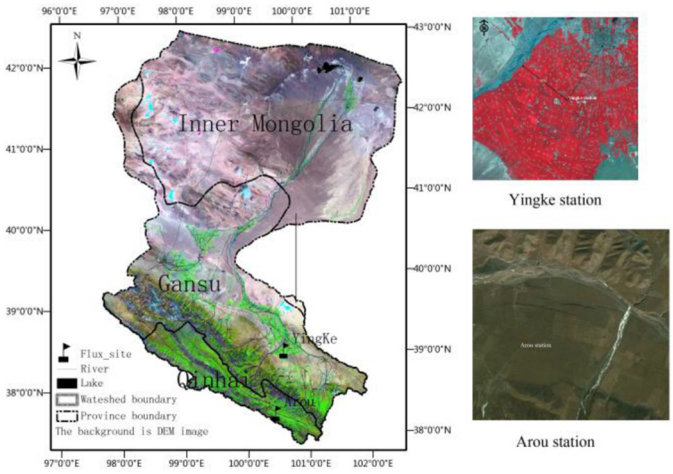

Fig. 1. Location of observation sites over the Heihe River Basin.

resistance. Mu proposed a restriction impedance function of temperature and vapor pressure deficit for estimation of the surface resistance [24]. Ortega-Farias showed that soil moisture content, net radiation, and vapor pressure deficit affect the estimation of surface resistance [12]. Irmak and Mutiibwa showed that wind speed, LAI, and canopy relative humidity also affect surface resistance [31]. Only some of these factors were considered in the estimation of daily ET in ETWATCH, an operational ET monitoring system incorporating remotely sensed data currently operating in the Heihe river basin in northern China [25], [26].

The purpose of this paper is to investigate an enhanced method, incorporating additional factors affecting surface resistance, for scaling satellite estimated ET on cloud-free days to a complete set of daily ET measures for the ETWatch system. Surface resistance is estimated based on the *P–M* equation with the introduction of radiation and meteorological information. The validation data are collected from the Heihe river basin in northern China, where a serious water resources' crisis over the last several years has intensified the need for this type of information. In the future, the method will scale to the estimation of regional daily ET map.

II. Study Site and Datasets

The Heihe river basin ($\sim 128\,900\ \mathrm{km}^2$), the second largest inland river basin in the country, is located in the arid northwest region of China between $97°24' - 102°10'$E and $37°41' - 42°42'$N. Its elevation ranges from approximately 5000 m in the upper reaches to 1000-m downstream. The river originates in the Qilian mountains and flows through the Hexi corridor of Gansu Province from the Yingluo Gorge, through the Zhengyi Gorge, and then northward into the Ejina oasis in the western part of the Inner-Mongolia plateau before finally discharging into the east and west Juyan lakes (Fig. 1).The landscape varies from glaciers and frozen soil to alpine meadow, forest, irrigated cropland, riparian ecosystem, bare gobi, and desert. A large proportion of the watershed area comprises sparse vegetation or bare land. The highest air temperatures are about 40 °C downstream in summer and the lowest fall to about -40 °C in the upper watershed in winter. The mean annual rainfall across the basin is 110.9 mm year^{-1} (1980–2010).

Because of scarce water resources in this basin, a large number of research projects in hydrology and water resources, environmental ecology, and land surface processes have been carried out since 1989, such as HEIFE [32], AECMP'95 [33], DHEX [34], WATER project [35], and Hi-WATER [36]. A large body of ground observations data from meteorological, hydrological, and energy flux stations and associated study results has been accumulated. This rich knowledge resource has laid the foundation for much scientific research on the Heihe river basin.

III. Methodology

A. Data and Preprocessing Methods

1) Field Observations: For this study, two ground observation stations in the Heihe River Basin were used: the Arou (AR) station and the Yingke (YK) station. The AR station ($100°27'53''$E, $38°02'40''$N) is located in the upper reaches of the Heihe River Basin in an east-west-oriented valley with a maximum width of 3 km from north to south. Average annual temperature is 0.9 °C, and annual precipitation is 403.1 mm (1960–2000). The terrain around the AR site is relatively flat, with a gentle decline from the southeast to the northwest. The underlying surface is natural pasture, and the vegetation is alpine meadow with the maximum height of the grass approximately 0.2–0.3 m during the growing season. The YK station ($100°24'37''$E, $38°51'26''$N) is in a typical oasis with very flat terrain, approximately 8 km southwest of Zhangye City. It is surrounded by the Gobi Desert, which commences approximately 7 km from the site. It is located in the middle reaches of the Heihe River Basin, and the main crops are maize; it has an average annual temperature of 7.2 °C and annual precipitation of 126.7 mm (1960–2000).

Each station is equipped with an EC tower and an automatic weather system (AWS). The EC system at AR station was installed in the center of the terrain (approximately 1300 m along a nearly flat terrain from south to north). The EC system at YK station was installed in an irrigated field. The EC sensors are installed at 2.81 m and 3.15 m above the ground at YK and AR, respectively. The EC data are sampled at a frequency of 10 Hz at both stations, and the turbulent fluxes (sensible heat flux and latent heat flux) are recorded by data loggers (Campbell Scientific, CR5000) with an average frequency of 30 min. The AWS systems collect data on air temperature, humidity, wind speed, wind direction, air pressure, precipitation, soil temperature and soil moisture profile, solar radiation, upward shortwave and longwave radiation, downward longwave radiation, and soil heat flux (Fig. 2), also recorded by data loggers (Campbell Scientific, CR800 at YK, CR23X at AR) at 10-min intervals. The data during rainfall events, instrument malfunctions and days of site inspection, and regular monthly maintenance of the sensors were omitted. The data used in the study include 2008 and 2010 due to data collection.

The EdiRe software (University of Edinburgh, http://geos.ed.ac.uk/abs/research/micromet/EdiRe) was used to process the

Instrument	Variable	Sensors		Height/Depth(m)		Landscape	
		YK	AR	YK	AR	YK	AR
EC	Sensible heat flux and latent heat flux	CSAT3, Campbell and Li7500, Li-cor	CSAT3, Campbell and KH2O, Campbell (11 Mar 2008–2 Apr 2008) CSAT3, Campbell and Li7500, Li-cor (10 Jun 2008–31 Dec 2009)	2.81	3.15		
AWS	Shortwave radiation	CM3,Kipp and Zonen	PSP,Eppley	4	1.5	Cropland (maize)	Alpine meadow
	Longwave radiation	CG3,Kipp and Zonen	PIP,Eppley	4	1.5		
	Air temperature	HMP45C	HMP45C	3.1	2.1		
	Air humidity	Vaisala	Vaisala	3.1	2.1		
	Wind speed	010C-1, Metone	014A, Metone	3.1	2.1		
	Air pressure	CS100,Campbell	CS105, Vaisala	–	–		
	Soil heat flux	HFP01,Hukeflux	HFT3,Campbell	0.05,0.15	0.05,0.15		
	Soil temperature	109,Campbell	107,Campbell	0.1,0.2,0.4 ,0.8,1.2,1.	0.1,0.2,0.4 ,0.8,1.2,1.		
	Soil moisture	CS616,Campbell	CS616,Campbell	0.1,0.2,0.4 ,0.8,1.2,1.	0.1,0.2,0.4 ,0.8,1.2,1.		
	Surface infrared thermometer	Campbell	–	6 4			
	Precipitation	52202, R.M.Yong	TE525,Campbell	–	–		

Fig. 2. Instrumentation at the YK and AR stations.

EC data on the two ground observation stations, including spike detection, lag correction of H_2O/CO_2 relative to the vertical wind component, sonic virtual temperature correction, rotation coordination using the planar fit method, correction for density fluctuation (WPL-correction), and frequency response correction [27], [37], [38].

2) MODIS and FY-2D/E Satellite Data: The MODIS 1B clear-sky data covering the Heihe River Basin were collected, which include 2008 and 2010. A geometric correction was performed using the built-in GCP point of the image to calculate the reflectance or radiance, which provided the calibration coefficients. Cloud pixels were detected using a method proposed by Ackerman that separates clear pixels from cloud-contaminated pixels using threshold values for multiple characteristics [39]. The NDVI in the experimental area was calculated using MODIS 1-, 2-band reflectivity after atmospheric correction. Surface albedo was computed from a linear combination of the first seven reflectance bands. Using MODIS data, 31-, 32-band radiance, and land surface temperature (night and day) were calculated using a split-window algorithm [40].

Cloud products covering the Heihe River Basin in 2008 and 2010 were obtained from the Chinese Meteorological Administration's (CMA) data services website in HDF format. A geographic lookup table (GLT) file downloaded from the National Satellite Meteorological Center was used to obtain the cloud classification data with 1-km resolution in a geographic projection for the target area. These data were generated by the FengYun-2D/E (FY-2D/E) satellites, the second and third operational vehicles of the first generation geostationary meteorological satellite system operated by the CMA, launched on December 8, 2006 and December 23, 2008, respectively, and they were located above the Equator at longitudes 86.5°E and 123.5°E at an altitude of 35 800 km. Their objective was to monitor clouds and temperature above China and neighboring areas of the Asia–Pacific region. The upgraded Stretched-Visible and Infrared Spin-Scan Radiometer (S-VISSR) is one of the major payloads onboard the FY-2D/E. This optical imaging radiometer consists of one visible channel with a resolution of 1.25 km and four infrared channels with a resolution of 5 km at wavelengths VIR: $0.55-0.90\mu$m, IR1: $10.3-11.3\mu$m, IR2: $11.5-12.5\mu$m, IR3: $6.3-7.6\mu$m, IR4: $3.5-4.0\mu$m. It can acquire one image per hour covering the Earth's surface from 60°N to 60°S and 45°E to 165°E.

3) Meteorological Data: Diurnal meteorological data in 2008 and 2010 are provided by China National Meteorological Bureau, including air temperature, air pressure, air humidity, and wind speed. For ET estimation, all variables were corrected for elevation above sea level and interpolated into a daily map at 1-km resolution. Inverse distance squared was used for air temperature and pressure interpolation, in combination with DEM data, and thin-plate splines were employed for other variables [41]. Instantaneous maps of air temperature were approximated from daily maximum air temperatures using a sine conversion.

4) Soil Moisture Content Data: Soil moisture content (high resolution, 1 km) in 2008 and 2010 used in this paper was retrieved from the Advanced Microwave Scanning Radiometer on Earth Observing system (AMSR-E) brightness temperatures and MODIS LST and NDVI Data, and the calculation includes two steps: the first step is to retrieve the high-resolution AMSR-E brightness temperature by downscaling passive microwave brightness temperature using high-resolution land surface temperature (MODIS LST) and MODIS NDVI data, and then the second step is to calculate the high-resolution soil moisture from high-resolution brightness temperature using the single-channel algorithm (SCA) and the Op model [42], [55]. The AMSR-E on the Aqua satellite is a passive microwave sensor which has been providing brightness temperature at five frequencies from 6.9 to 89 GHz since 2002. AMSR-E C-band channels are suitable for soil moisture remote sensing [43]. AMSR-E/NSIDC products Level-3 B02 are used in this study. They are provided on a 25-km regular grid. Soil moisture is obtained from an iterative inversion algorithm using 10.7- and 18.7-GHz data, although this algorithm was initially developed for 6.9- and 10.7-GHz frequencies [43].

5) Surface Net Radiation Data: Surface net radiation is the energy source for ET, controlling the sensible heat flux, latent heat flux, and soil heat flux. Currently, ETWatch calculates daily net radiation using the traditional method recommended by the FAO for meteorological data [44]. Spatial variation in this measure is affected by the spatial interpolation of the meteorological data, especially for sunshine. Its accuracy is limited by the number and location of meteorological stations. For this study, cloud data from the FY-2D/E satellite were used instead of the interpolated sunshine data in ETWatch to estimate the daily net radiation at 1-km resolution [45]. This approach should provide a better estimate of the spatial variation of net radiation.

B. Conversion Methodology

ETWatch uses an integration of the "residue approach" and the $P-M$ model for ET estimation [25]–[27], [46]. The residue approach is an energy balance model which combines the existing SEBS and SEBAL models and the mass transfer method. It computes ET for cropped surfaces from standard meteorological records of sunshine, temperature, humidity, and wind speed by introducing resistance factors. The *P–M* model determines the spatiotemporal variability of regional evaporative

conditions using the available surface resistance (r_s) as the temporal scaling factor. When the bulk surface resistance is properly defined, the $P-M$ equation is valid for calculating daily ET for both soil and vegetation canopies and then aggregating it to monthly and annual ET computed from spectral radiances on cloud-free days. $P-M$ equation used is

$$\lambda LE = \frac{\Delta\left(R_n - G\right) + \rho_a C_p \frac{(e_s - e_a)}{r_a}}{\Delta + \gamma\left(1 + \frac{r_s}{r_a}\right)} \tag{1}$$

where r_s is the surface resistance, LE represents daily ET, R_n is the net radiation, G is the soil heat flux, $(e_s - e_a)$ is the vapor pressure deficit of the air, ρ_a is the mean air density at constant pressure, C_p is the specific heat of the air, Δ is the slope of the saturation vapor pressure temperature relationship, γ is the psychometric constant, and r_a is the aerodynamic resistance.

If the daily surface resistance on the regional scale is known, the daily ET can be estimated at on the regional scale from (1).

1) Enhanced Surface Resistance Approach: In ETWatch, the conversion of ET on cloud-free days into daily ET relies on surface resistance (r_s) extended from r_s on the closest cloud-free day [25]–[27], smoothed LAI values, soil moisture content, and daily constraints functions for stomatal aperture response to minimum air temperature $m(T_{min})$ and vapor pressure deficit $m(VPD)$. The quadratic equation used is

$$\begin{aligned} r_{s,daily} &= \frac{r_{\min,daily}}{LAI_{daily} \cdot SM_{daily}} \\ &= \frac{r_{\min,clear} \times LAI_{clear} \times SM_{clear}}{LAI_{daily} \times m\left(T_{\min}\right) \times m\left(VPD\right) \times SM_{daily}} \end{aligned} \tag{2}$$

where is $r_{min,daily}$ is the daily bulk stomatal resistance of a well-illuminated leaf, LAI_{daily} is a daily dataset of leaf area index values smoothed by a Savitzky–Golay filter [47], SM_{daily} is daily soil moisture content retrieved from the AMSR-E microwave brightness temperature [42], [55], $r_{min,clear}$ is the bulk stomatal resistance of a well-illuminated leaf on the clear day, LAI_{clear} is LAI calculated using the clear-day satellite data, and SM_{clear} is the soil moisture content retrieved from AMSR-E on the clear day.

This paper explores alternative formulations for (1), including the effectiveness of currently used variables such as $m(T_{min}), m(VPD)$, and soil moisture content; and the possible use of new measures such as net radiation, wind velocity, relative humidity, and the actual vapor pressure. To assess their effectiveness, each variable was included individually as in (3). The reconstructed surface resistance was then used to re-estimate the daily ET in ETWatch and compared with actual ET measurements.

$$r_{s,daily} = \frac{r_{\min,daily}}{LAI_{daily} f(s)} = \frac{r_{\min,clear} \times LAI_{clear} \times f(s)}{LAI_{daily} \times f(s)} \tag{3}$$

where $f(s)$ represents any one of the alternative variables.

C. Assessment

Effectiveness is assessed based on some widely used goodness-of-fit statistics [48], specifically the coefficient of determination (R_2), index of agreement (d), mean absolute error (MAE), and root-mean-square error $(RMSE)$, defined as

$$R^2 = \frac{\left[\sum_{i=1}^{n}\left(O_i - \bar{O}\right)\left(P_i - \bar{P}\right)\right]^2}{\left[\sum_{i=1}^{n}\left(O_i - \bar{O}\right)^2 \sum_{i=1}^{n}\left(P_i - \bar{P}\right)^2\right]} \tag{4}$$

$$MAE = n^{-1}\sum_{i=1}^{n}\left|P_i - O_i\right| \tag{5}$$

$$RMSE = \sqrt{n^{-1}\sum_{i=1}^{n}\left(P_i - O_i\right)^2} \tag{6}$$

$$d = 1 - \frac{\sum_{i=1}^{n}\left(P_i - O_i\right)^2}{\sum_{i=1}^{n}\left(\left|P_i - \bar{O}\right| + \left|O_i - \bar{O}\right|\right)^2} \tag{7}$$

where O_i is the actual measurement and P_i is its estimate, $\bar{O}$ is the mean measurement, $\bar{P}$ is the mean of the estimates, and n is the sample size. Colaizzi and Liu suggest as follows: 1) the method performs well when the MAE is less than 50% of the measured standard deviation; 2) there are few outliers when $RMSE$ is not greater than 50% of MAE; and 3) the closer d is to 1, the better the model performance [11], [50].

TABLE I
STATISTICS FOR THE PERFORMANCE OF SURFACE RESISTANCE AFTER THE INTRODUCTION OF ALTERNATIVE VARIABLES

Environmental factors	Station	Correlation equation	R^2
ETWatch_original	YK	y = 1.2097x – 0.3668	0.84
	AR	y = 1.1745x – 0.3347	0.83
m(T_{min}) and *m(VPD)* (Constraints function)	YK	y = 0.9489x + 0.0938	0.78
	AR	y = 0.9734x + 0.3528	0.73
Net radiation	YK	y = 0.9527x – 0.0576	0.91
	AR	y = 0.9738x + 0.1764	0.91
Soil moisture content	YK	y = 0.9707x + 0.0092	0.91
	AR	y = 0.973x + 0.287	0.89
Vapor pressure deficit (VPD)	YK	y = 0.9725x – 0.0696	0.88
	AR	y = 0.9902x + 0.1489	0.89
Wind speed	YK	y = 1.0085x + 0.0054	0.92
	AR	y = 1.0105x + 0.2593	0.89
Relative humidity	YK	y = 0.9631x + 0.0415	0.9
	AR	y = 0.9629x + 0.3199	0.87
Actual vapor pressure	YK	y = 0.9734x + 0.0198	0.89
	AR	y = 0.9797x + 0.2673	0.88

IV. RESULTS

Table I contains the statistics on model performance after the introduction of each alternative environmental variable in 2008 and 2010. The currently used climatic factors have a lesser

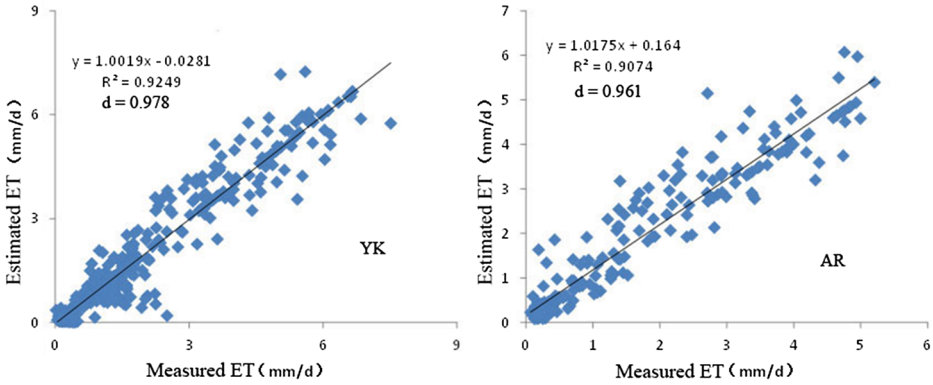

Fig. 3. Results of re-estimating ET based on the enhanced model for YK and AR stations.

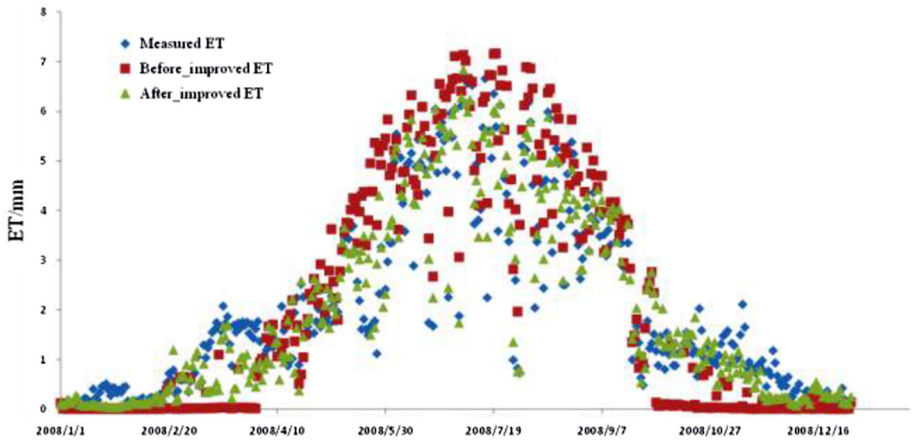

Fig. 4. Change over time for ET estimates based on the original and enhanced models.

effect on ET than some of the possible new measures. Factors with a greater degree of influence, indicated by their higher R^2 values, are net radiation, soil moisture, and wind speed; those with a lesser influence are $m(T_{min})$ and $m(VPD)$ which are used in the current model.

Based on these results, the gap-filling surface resistance estimation was modified to include only those climatic factors having the greatest influence, specifically wind speed, soil moisture, and net radiation, resulting in the following equation:

$$r_{s,daily} = \frac{r_{\min,clear} \times LAI_{clear} \times Rn_{clear} \times SM_{clear} \times U_{clear}}{LAI_{daily} \times SM_{daily} \times Rn_{daily} \times U_{daily}} \tag{8}$$

where SM_{daily} is daily soil moisture content retrieved from AMSR-E microwave brightness temperature, Rn_{daily} is daily net radiation retrieved from FY-2 cloud products data and meteorological data interpolated into a daily map, Rn_{clear} is the net radiation on a clear day, U_{daily} is daily wind speed data from interpolation of the meteorological data, and U_{clear} is wind speed data on a clear day. Other variables are as defined for (2).

Fig. 3 shows the results of re-estimating ET based on the improved surface resistance measure incorporating net radiation, soil moisture, and wind speed in 2008 and 2010. For the upstream AR alpine meadow area (grassland), the coefficient of determination (R^2) is 0.9074, which indicates a strong correlation between actual ET and ET estimated by the improved surface resistance method; the d is 0.961, again suggesting good performance. For the midstream YK oasis plains area (maize cropland), the coefficient of determination (R^2) is 0.9249, again indicating a strong correlation between actual ET and ET estimated by the improved method. The RMSE is 0.5288, and the difference between $RMSE$ and MAE is less than 40% of MAE, meaning there are few outliers in the estimated ET according to Colaizzi [11]. The d is 0.978, also suggesting good performance. Both coefficients of determination are higher than the corresponding coefficients for the original model used in ETWatch, which were 0.84 and 0.83, respectively (Table I). Both the original model and enhanced models give slightly better predictions in the cropland region (YK station) than the grassland region (AR station).

To explore seasonal variability, Fig. 4 shows the daily values for 2008 of measured ET compared with ET estimated by the original and the enhanced models for the YK station. Fig. 5 shows the absolute values of the residuals between measured ET and ET estimated by the original and enhanced models, averaged by month. The residuals are consistently smaller every month for the enhanced model, demonstrating the superiority of the new approach. Fig. 6 shows the absolute difference between the residuals of the original and enhanced models, as a percentage of the measured ET. This provides a measure of the degree to which the enhanced model improves upon the original relative to the magnitude of the value being estimated.

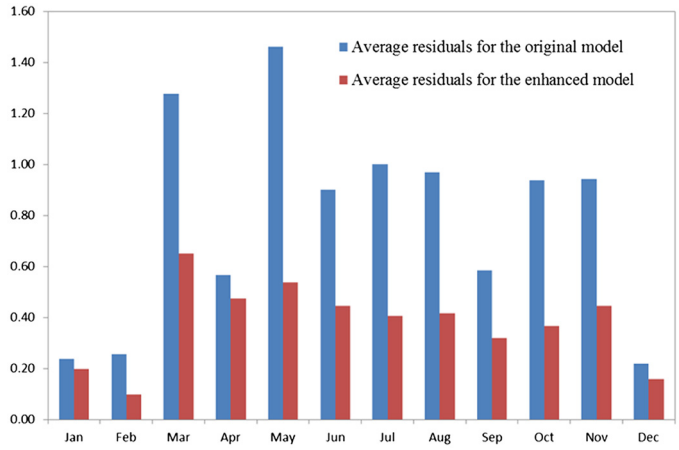

Fig. 5. Average absolute residuals for the original and enhanced models by month.

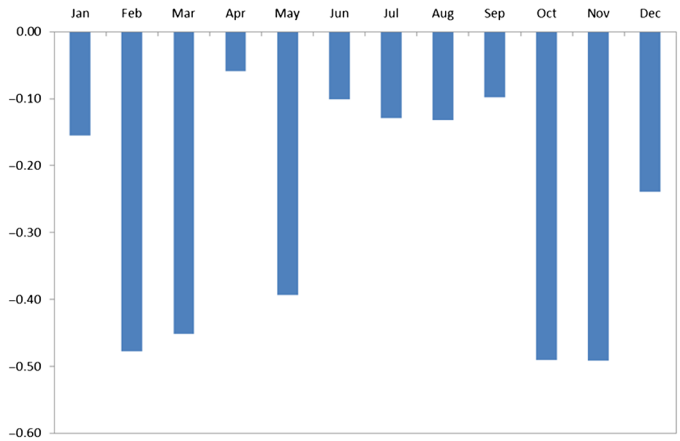

Fig. 6. Difference between residuals of the original and enhanced models as percent of measured ET.

Particularly in late winter/early spring (February/March and May), and in fall (October/November), the ET estimation based on the enhanced surface resistance estimation method is significantly improved over the original model. Residuals were reduced by almost 50% of the magnitude being estimated. This may be a result of including wind speed in the model which is more prevalent in the spring and fall seasons, and there is less vegetation to prevent evaporation from soils. Estimates for April from the enhanced model are consistent with the March and May estimates but appear to be an outlier in Fig. 6 only because the original model provided a better estimate in April than it did in the other months.

V. Discussion

Surface resistance is a key parameter in the process of ET estimation and is affected by the underlying surface and climatic factors. Since vegetation coverage is smaller in winter, spring, and fall in the Heihe river basin, more factors need to be considered in gap-filling surface resistance. The energy involved with ET affects net radiation. Wind speed reflects energy transferred by advection from adjacent areas, and soil moisture content can suggest evaporative capacity and the effects of human activities. Consequently, incorporating these factors into an improved surface resistance measure should provide a better estimate of ET.

The method discussed here relies upon discrete georeferenced area-scaled pixels. For MODIS data, the pixel value represents the average surface soil heat flux for a 1 km x1 km area. Ground station measurements of ET represent a different area; usually only within the range of a few hundred square meters of the EC towers from which the *in situ* data are collected. This does not match the area covered by a pixel. Consequently, some outliers would be expected in Fig. 4 where estimated ET is compared with measured *in situ* ET. This issue of mismatching scales is especially problematic for areas with heterogeneous terrain, land use, and climate conditions. Fortunately, the underlying surfaces are relatively homogeneous at those two test stations; thus, the *in situ* ground measurements used for validation should approximate conditions over the entire pixel measured by the satellite.

Many studies mention that ET measured by an EC system over irrigated regions is subject to considerable uncertainty [27], [51]–[54], and in particular, measured ET is usually greater than the ET estimated from satellite data. In addition to the issue of mismatching scales, there are a variety of reasons for this including different footprints, advection, calibration of sensors, and loss between low-frequency and high-frequency measurements from EC data. The results from the enhanced model are consistent with this; the average measured ET values (2.03) are slightly greater than the values estimated from the satellite data (2.01).

Other weak elements of the research include the use of net radiation from the FY-2 geostationary meteorological satellite cloud products data, and wind speed data from the interpolation of ground-based meteorological data. The FY-2 data are 5 km, whereas the MODIS data are 1 km. Not only the soil moisture and cloud covering data are spatially coarse, but the different spatial scales of all three will affect the results of the ET estimation. Also, the number of ground meteorological stations and the geostatistical procedure used for interpolation will affect wind speed measures. Further research is clearly needed to downscale the cloud data to support the development of high-precision region-wide ET data.

VI. Conclusion

In this study, we demonstrated an improved method based on surface resistance for converting satellite ET measures on clear, cloud-free days into ET estimates for all days. The study was conducted in the Heihe river basin area of northern China. It uses daily net radiation, soil moisture, and wind speed, which were shown to be the most important factors for surface resistance, to estimate daily surface resistance, and then combines them with meteorological data using the $P-M$ model to estimate daily ET. High correlations were obtained between the estimated and *in situ* measured ET at both the YK station (coefficient of determination, $R^2 = 0.9249$ and index of agreement, $d = 0.978$) and the AR station (coefficient of determination, $R^2 = 0.9074$ and index of agreement $d = 0.961$) in 2008. These coefficients of determination for the enhanced model

were higher than those for the original model. It was also shown that the enhanced model provided improved results for every month of the year but especially in late winter/early spring and autumn. Incorporating this enhanced model into ETWatch should provide superior ET estimates for this system and for any other application requiring daily ET estimates and/or the accumulation of daily estimates into totals on a regional scale for a specified time period. Such accumulated values are critical, for example, for water use planning, especially in arid and semiarid areas. The ready availability of the satellite data from which these estimates are derived makes ET estimation possible in these areas without the need for expensive *in situ* ET measurement instrumentation. In the future, this method will be applied to the estimation of regional daily ET map.

ACKNOWLEDGMENT

The authors would like to thank the Environmental and Ecological Science Data Center for West China, National Natural Science Foundation of China for providing the ground observations data (http://westdc.westgis.ac.cn); the China Meteorological Data Sharing Service System for providing the Meteorological data (http://cdc.cma.gov.cn/cdc_en/home.dd); NASA Goddard Space Flight Center (GSFC) Distributed Active Archive Center (GDAAC) for providing the MODIS data (http://reverb.echo.nasa.gov/reverb/); and the National Satellite Meteorological Center for providing the FY-2D/E satellite data (http://fy3.satellite.cma.gov.cn/portalsite/default.aspx?currentculture=en-US).The authors also appreciate the comments and suggestions by Prof. R. Briggs on earlier versions of this paper.

REFERENCES

[1] B. F. Wu, L. P. Jiang, N. N. Yan, C. Perry, and H. W. Zeng, "Basin-wide evapotranspiration management: Concept and practical application in Hai Basin, China," *Agric. Water Manage.*, vol. 145, pp. 145–153, Nov. 2014.

[2] H. Bormann, "Sensitivity analysis of 18 different potential evapotranspiration models to observed climatic change at German climate stations," *Clim. Change*, vol. 104, no. 3–4, pp. 729–753, Feb. 2011.

[3] R. Qiu *et al.*, "Energy partition and evapotranspiration of hot pepper grown in greenhouse with furrow and drip irrigation methods," *Sci. Hortic.*, vol. 129, no. 4, pp. 790–797, Jul. 2011.

[4] P. Bhantana and N. Lazarovitch, "Evapotranspiration, crop coefficient and growth of two young pomegranate (Punica granatum L.) varieties under salt stress," *Agric. Water Manage.*, vol. 97, no. 5, pp. 715–722, May 2010.

[5] B. Zhang, S. Kang, F. Li, and L. Zhang, "Comparison of three evapotranspiration models to Bowen ratio-energy balance method for a vineyard in an arid desert region of northwest China," *Agric. For. Meteorol.*, vol. 148, no. 10, pp. 1629–1640, Sep. 2008.

[6] W. A. Dugas *et al.*, "Bowen ratio, eddy correlation and portable chamber measurements of sensible and latent heat flux over irrigated spring wheat," *Agric. For. Meteorol.*, vol. 56, no. 1–2, pp. 1–20, Jul. 1991.

[7] W. M. L. Meijninger and H. A. R. De Bruin, "The sensible heat fluxes over irrigated areas in western turkey determined with a large aperture scintillometer," *J. Hydrol.*, vol. 229, no. 1–2, pp. 42–49, Mar. 2000.

[8] F. Casterllvi and R. L. Snyder, "A new procedure based on surface renewal analysis to estimate sensible heat flux: A case study over grapevines," *J. Hydrometeorol.*, vol. 11, no. 2, pp. 496–508, Apr. 2010.

[9] R. D. Jackson, J. L. Hatfield, R. J. Reginato, S. B. Idso, and P. J. Pinter, "Estimation of daily evapotranspiration from one time-of-day measurements," *Agric. Water Manage.*, vol. 7, no. 1–3, 30, pp. 351–362, Sep. 1983.

[10] M. Tasumi, R. Trezza, R. G. Allen, and J. L. Wright, "Operational aspects of satellite based energy balance models for irrigated crop in the semi-arid US," *Irrig. Drain. Syst.*, vol. 19, no. 3–4, pp. 355–376, Nov. 2005.

[11] P. D. Colaizzi, S. R. Evett, T. A. Howell, and J. A. Tolk, "Comparison of five models to scale daily evapotranspiration from one-time-of-day measurements," *Trans. ASAE*, vol. 49, no. 5, pp. 1409–1417, Jul. 2006.

[12] S. Ortega-Farias, A. Olioso, R. Antonioletti, and N. Brisson, "Evaluation of the penman–monteith model for estimating soybean evapotranspiration," *Irrig. Sci.*, vol. 23, no. 1, pp. 1–9, Apr. 2004.

[13] J. L. Chavez, C. M. U. Neale, J. H. Prueger, and W. P. Kustas, "Daily evapotranspiration estimates from extrapolating instantaneous airborne remote sensing ET values," *Irrig. Sci.*, vol 27, no. 1, pp. 67–81, Nov. 2008.

[14] M. Todorovic, "Single-layer evapotranspiration model with variable canopy resistance," *J. Irrig. Drain. Eng.*, vol. 125, no. 5, pp. 235–245, Oct. 1999.

[15] P. Steduto, M. Todorovic, A. Caliandro, and P. Rubino, "Daily reference evapotranspiration estimates by the penman–monteith equation in southern italy. constant vs. variable canopy resistance," *Theor. Appl. Climatol.*, vol. 74, no. 3–4, pp. 217–225. Mar. 2003.

[16] S. Lecina, A. M. Cob, P. J. Perez, F. J. Villalobos, and J. J. Baselga, "Fixed versus variable bulk canopy resistance for reference evapotranspiration estimation using the Penman–Monteith equation under semiarid conditions," *Agric. Water Manage.*, vol. 60, no. 3, pp. 181–198, May 2003.

[17] P. J. Perez, S. Lecina, F. Castellvi, A. M. Cob, and F. J. Villalobos, "A simple parameterization of bulk canopy resistance from climatic variables for estimating hourly evapotranspiration," *Hydrol. Process.*, vol. 20, no. 3, pp. 515–532, Feb. 2006.

[18] W. J. Shuttleworth, R. J. Gurney, A. Y. Hsu, and J. P. Ormsby, "FIFE: The variation in energy partition at surface flux sites," *IAHS Publ.*, vol. 186, pp. 67–74, May 1989.

[19] R. Crago and W. Brutsaert, "Daytime evaporation and the self-preservation of the evaporative fraction and the Bowen ratio," *J. Hydrol.*, vol. 178, no. 1–4, pp. 241–255, Apr. 1996.

[20] J. Jiang, Y. Zhang, and C. Liu, "Estimation of regional evapotranspiration using high resolution LANDSAT/ETM+ data," *Adv. Water Sci.*, vol. 16, no. 2, pp. 274–279, Mar. 2005

[21] J. C. B. Hoedjes, A. Chehbouni, F. Jacob, J. Ezzahar, and G. Boulet, "Deriving daily evapotranspiration from remotely sensed instantaneous evaporative fraction over olive orchard in semi-arid Morocco," *J. Hydrol.*, vol. 354, no. 1–4, pp. 53–64, Jun. 2008.

[22] S. Li, S. Kang, F. Li, L. Zhang, and B. Zhang, "Vineyard evaporative fraction based on eddy covariance in an arid desert region of Northwest China," *Agric. Water Manage.*, vol. 95, no. 8, pp. 937–948, Aug. 2008.

[23] L. Testi, F. Orgaz, and F. J. Villalobos, "Variations in bulk canopy conductance of an irrigated olive (Olea europaea L.) orchard," *Environ. Exp. Bot.*, vol. 55, no. 1–2, pp. 15–28, Jan. 2006.

[24] Q. Z. Mu, A. H. Faith, M. S. Zhao, and W. R. Steven, "Development of a global evapotranspiration algorithm based on MODIS and global meteorology data," *Remote Sen. Environ.*, vol. 111, no. 4, pp. 519–536, Dec. 2007.

[25] B. F. Wu, J. Xiong, and N. N. Yan, "ETWatch: An operational ET monitoring system with remote sensing," ISPRS III Workshop, presented at the ISPRS Workshop on Geoinformation and Decision Support Systems, Tehran, Iran, 6–7 Jan. 2008.

[26] B. F. Wu, J. Xiong, M. G. Hu, N. N. Yan, and L. D. Yang, "ETWatch for monitoring regional evapotranspiration with remote sensing," *Adv. Water Sci.*, vol. 19, no. 5, pp. 671–678, Sep. 2008.

[27] B. F. Wu, N. N. Yan, J. Xiong, W. G. M. Bastiaanssen, W. W. Zhu, and A. Stein, "Validation of ETWatch using field measurements at diverse landscapes: A case study in Hai Basin of China," *J. Hydrol.*, vol. 436–437, pp. 67–80, May 2012.

[28] H. O. Farah, "Estimation of regional evaporation under different weather conditions from satellite and meteorological data, a case study in the naivasha basin," Ph.D. Thesis, Wageningen Univ., Wagenigen, The Netherlands, pp. 170, 2001.

[29] H. A. Cleugh, R. Leuninga, Q. Z. Mu, and S. W. Running, "Regional evaporation estimates from flux tower and MODIS satellite data," *Remote Sens. Environ.*, vol. 106, no. 3, pp. 285–304, Feb. 2007.

[30] A. H. Teixeira de Castro, M. D. Ahmad, and M. G. Bos, "Reviewing SEBAL input parameters for assessing evapotranspiration and water productivity for the low-middle Sao Francisco river basin, Brazil, part a: Calibration and validation," *Agric. For. Meteorol.*, vol. 149, no. 3–4, pp. 462–476, Mar. 2008.

[31] S. Irmak and D. Mutiibwa, "On the dynamics of canopy resistance: Generalized linear estimation and relationships with primary micrometeorological variables," *Water Resour. Res.*, vol. 46, no. 8, pp. W08526, Aug. 2010.

[32] Y. Gao and Y. Hu, *Advances in HEIFE Research (1987–1994)*, Special Issue 1st ed. Beijing, China: China Meteorological Press, 1994, p. 191.

[33] Y. M. Ma *et al.*, "Satellite remote sensing parameterization of regional land surface heat fluxes over heterogeneous surface of arid and semi-arid areas," *Plateau Meteorol.*, vol. 23, no. 2, pp. 139–146, Apr. 2004.
[34] Y. M. Ma, W. Q. Ma, M. S. Li, F. L. Sun, and J. M. Wang, "Remote sensing parameterization of land surface heat fluxes over the middle reaches of the Heihe River," *J. Desert Res.*, vol. 24, no. 4, pp. 392–401, Jul. 2004.
[35] X. Li *et al.*, "Watershed allied telemetry experimental research," *J. Geophys. Res.-Atmos.*, vol. 114, p. D22103, Nov. 2009.
[36] X. Li *et al.*, "Heihe watershed allied telemetry experimental research (HiWATER): Scientific objectives and experimental design1," *Bull. Amer. Meteorol. Soc.*, vol. 94, no. 8, pp. 1145–1160, Aug. 2013.
[37] P. D. Blanken *et al.*, "Turbulence flux measurements above and below the overstory of a boreal aspen forest," *Bound.-Lay. Meteorol.*, vol. 89, pp. 109–140, Oct. 1998.
[38] S. M. Liu *et al.*, "A comparison of eddy-covariance and large aperture scintillometer measurements with respect to the energy balance closure problem," *Hydrol. Earth Syst. Sci.*, vol. 15, pp. 1291–1306, 2011.
[39] A. Steve *et al.*, (2016, Oct.). "Discriminating clear-sky from cloud with MODIS algorithm theoretical basis document (Mod35), Version 5.0" [Online]. Available: http://citeseerx.ist.psu.edu/viewdoc/download?doi=10.1.1.385.7073&rep=rep1&type=pdf
[40] L. P. Jiang, Z. H. Qin, and W. Xie, "Program splits window algorithm to retrieve land surface temperature for MODIS data using IDL," *Geomatics Spatial Inf. Technol.*, vol. 29, no. 3, pp. 114–117, 2006.
[41] Q. J. Qian, B. F. Wu, and J. Xiong, "Interpolation system for generating meteorological surfaces using to compute evapotranspiration in Haihe River Basin," in *Proc. 2005 IEEE Int. Geosci. Remote Sens. Symp. (IGRASS'05)*, Jul. 2005, vol. 1, pp. 616–619.
[42] C. Gruhier *et al.*, "Evaluation of AMSR-E soil moisture product based on ground measurements over temperate and semi-arid regions," *Geophys. Res. Lett.*, vol. 35, no. 10. p. L10405 May 2008.
[43] E. Njoku, T. Jackson, V. Lakshmi, T. Chan, and S. Nghiem, "Soil moisture retrieval from AMSR-E," *IEEE Geosci. Remote Sens. Lett.*, vol. 41, no. 2, pp. 215–229, Feb. 2003.
[44] R. Allen, L. Pereira, D. Raes, and M. Smith, "Crop evapotranspiration-Guidelines for computing crop water requirements," FAO Irrigation and Drainage Paper, 1998, p. 56.
[45] S. F. Liu, "Research on land surface net radiation remote sensing estimation," Ph.D. dissertation, Inst. Remote Sens. Digital Earth, Univ. of Chinese Academy of Sciences,, Beijing, China, May 2013.
[46] J. Xiong, B. F. Wu, N. N. Yan, Y. Zeng, and S. F. Liu, "Estimation and validation of land surface evaporation using remote sensing and meteorological data in North China," *IEEE J. Sel. Top. Appl. Earth Observ. Remote Sens.*, vol. 3, no. 3, pp. 337–344, Sep. 2010.
[47] J. Chen, P. Jonsson, M. Tamura, Z. H. Gu, B. Matsushita, and L. Eklundh, "A simple method for reconstructing a high-quality NDVI time series dataset based on the Savitky-Golay filter," *Remote. Sens. Environ.*, vol. 91, pp. 332–344, Mar. 2004.
[48] J. Cai, Y. Liu, T. Lei, and L. S. Pereira, "Estimating reference evapotranspiration with the FAO Penman–Monteith equation using daily weather forecast messages," *Agric. For. Meteorol.*, vol. 145, no. 1–2, pp. 22–35, Jul. 2007.
[49] G. S. Liu, M. Hafeez, Y. Liu, D. Xu, and C. Vote, "Comparison of two methods to derive time series of actual evapotranspiration using eddy covariance measurements in the southeastern Australia," *J. Hydrol.*, vol. 454–455, pp. 1–6, Aug. 2012.
[50] G. S. Liu, M. Hafeez, Y. Liu, D. Xu, and C. Vote, "A novel method to convert daytime evapotranspiration into daily evapotranspiration based on variable canopy resistance," *J. Hydrol.*, vol. 414–415, pp. 278–283, Jan. 2012.
[51] J. M. Norman, W. P. Kustas, and K. S. Humes, "Source approach for estimating soil and vegetation energy fluxes in observations of directional radiometric surface temperature," *Agric. For. Meteorol.*, vol. 77, no. 3–4, pp. 263–293, Dec. 1995.
[52] K. Wilson *et al.*, "Energy balance closure at Fluxnet sites," *Agric. For. Meteorol.*, vol. 113, no. 1–4, pp. 223–243, Dec. 2002.
[53] A. H. De. C. Teixeira and W. G. M. Bastiaanssen, "Five methods to interpret field measurements of energy fluxes over a micro-sprinkler irrigated mango orchard," *Irrig. Sci.*, vol. 30, no. 1, pp. 13–28, Jan. 2012.
[54] Z. Z. Jia, S. M. Liu, Z. W. Xu, Y. J. Chen, and M. J. Zhu, "Validation of remotely sensed evapotranspiration over the Hai River Basin, China," *J. Geophys. Res. Atmos.*, vol. 117, p. D13113, Jul. 2012.
[55] C. Y. Song, L. Jia, and M. Menenti, "Retrieving high-resolution surface soil moisture by downscaling AMSR-E brightness temperature using MODIS LST and NDVI data," *IEEE J. Sel. Top. Appl. Earth Observ. Remote Sens.*, vol. 7, no. 3, pp. 935–942, Mar. 2014.

Bingfang Wu received the M.S. degree in water resources and system analysis from Tianjin University, Tianjin, China, and the Ph.D. degree in environmental planning and management from Tsinghua University, Tsinghua, China, in 1985 and 1989, respectively.

Currently, he is a Professor with the Institute of Remote Sensing and Digital Earth (RADI), Chinese Academy of Sciences (CAS), Beijing, China. He is the Co-Chair of the GEO/GEOSS Global Agricultural Monitoring Task. He has authored more than 300 papers and has written 2 books. His research interests include water resources monitoring, crop monitoring with remote sensing, and regional/global ecoenvironment evaluation.

Weiwei Zhu received the B.S. degree in surveying and mapping engineering from Central South University (CSU), Changsha, Hunan, China, and the Ph.D. degree in cartography and geography information system from the Institute of Remote Sensing and Digital Earth (RADI), Chinese Academy of Sciences (CAS), Beijing, China, in 2009 and 2014, respectively.

His research interests include land surface soil heat flux and net radiation estimation and ET modeling using remote sensing.

Nana Yan received the B.S. degree in information management from China Agriculture University, Beijing, China, and the Ph.D. degree in cartography and geography information system from the Institute of Remote Sensing and Digital Earth (RADI), Chinese Academy of Sciences (CAS), Beijing, China, in 2002 and 2013, respectively.

Her research interests include water resources and drought monitoring using remote sensing.

Xueliang Feng received the B.S. degree in hydrology and water resources engineering from Hohai University, Nanjing, China, in 2010. He is currently working toward the Ph.D. degree in cartography and geography information system at the Institute of Remote Sensing and Digital Earth (RADI), Chinese Academy of Sciences (CAS), Beijing, China.

His research interests include atmospheric boundary layer height estimation using remote sensing.

Qiang Xing received the B.S. degree in surveying and mapping engineering from Shandong University of Science and Technology, Qingdao, China, and the Ph.D. degree in cartography and geography information system from the Institute of Remote Sensing and Digital Earth (RADI), Chinese Academy of Sciences (CAS), Beijing, China, in 2006 and 2011, respectively.

His research interests include aerodynamic roughness estimation using microwave and optics remote sensing.

Qifeng Zhuang received the B.S. degree in geography information system from Nanjing Normal University, Nanjing, China, in 2011. He is currently working toward the Ph.D. degree in cartography and geography information system at the Institute of Remote Sensing and Digital Earth (RADI), Chinese Academy of Sciences (CAS), Beijing, China.

His research interests include sensible heat flux estimation and ET modeling using remote sensing.